Op18/stathmin Mediates Multiple Region-specific Tubulin and Microtubule-regulating Activities

Niklas Larsson,* Bo Segerman,* Bonnie Howell,‡ Kajsa Fridell,* Lynne Cassimeris,‡ and Martin Gullberg*

*Department of Cell and Molecular Biology, University of Umeå, Sweden; and ‡Department of Biological Sciences, Lehigh University, Bethlehem, Pennsylvania

Abstract. Oncoprotein18/stathmin (Op18) is a regulator of microtubule (MT) dynamics that binds tubulin heterodimers and destabilizes MTs by promoting catastrophes (i.e., transitions from growing to shrinking MTs). Here, we have performed a deletion analysis to mechanistically dissect Op18 with respect to (a) modulation of tubulin GTP hydrolysis and exchange, (b) tubulin binding in vitro, and (c) tubulin association and MT-regulating activities in intact cells. The data reveal distinct types of region-specific Op18 modulation of tubulin GTP metabolism, namely inhibition of nucleotide exchange and stimulation or inhibition of GTP hydrolysis. These regulatory activities are mediated via two-site cooperative binding to tubulin by multiple nonessential physically separated regions of Op18. In vitro analysis revealed that NH_2- and COOH-terminal truncations of Op18 have opposite effects on the rates of tubulin GTP hydrolysis. Transfection of human leukemia cells with these two types of mutants result in similar decrease of MT content, which in both cases appeared independent of a simple tubulin sequestering mechanism. However, the NH_2- and COOH-terminal–truncated Op18 mutants regulate MTs by distinct mechanisms as evidenced by morphological analysis of microinjected newt lung cells. Hence, mutant analysis shows that Op18 has the potential to regulate tubulin/MTs by more than one specific mechanism.

Key words: microtubules • phosphoproteins • phenotype • signal transduction • GTP phosphohydrolase

MICROTUBULES (MTs)[1] are ever changing dynamic structures that switch abruptly between growth and shortening by events called catastrophes, and vice versa by rescue events, a behavior called dynamic instability. MTs utilize polymerization-induced GTP hydrolysis to generate dynamic instability, and the tip of a polymerizing MT is thought to contain a stabilizing cap of GTP tubulin, the loss of which results in depolymerization, i.e., a catastrophe. Massive MT reorganization occurs during cell division, cell differentiation, and upon cytotoxic T cell recognition of its target cell (for review see Desai and Mitchison, 1997). MTs also act as an intracellular scaffold for a multitude of protein kinases and other signaling proteins, suggesting that regulation of dynamic instability in response to specific stimulation could be important for localizing signal transducing proteins (for review see Gundersen and Cook, 1999). Classically, regulation of MT dynamics has been ascribed to a class of nonmotor proteins collectively termed MT-associated proteins but more recently, oncoprotein 18/stathmin (Op18) has been identified as a regulator of MT dynamics both in vitro and in intact cells (for review see Cassimeris, 1999).

The MT destabilizing activity of Op18 is turned off in response to phosphorylation of four serine residues by both cell cycle– and cell surface receptor–regulated kinase systems (for review see Deacon et al., 1999). The phenotype of kinase target sites–deficient Op18 mutants in human cell lines show that phosphorylation downregulation is essential to allow microtubules to segregate condensed chromosomes (Marklund et al., 1994, 1996; Larsson et al., 1995). Functional inactivation by extensive mitotic phosphorylation argues against a functional role of Op18 during mitosis (Larsson et al., 1997). Rather, the high stoichiometry of Op18 phosphorylation by several receptor-regulated kinase systems suggests that the primary role for Op18 may be to regulate the MT system in response to external signals in interphase cells. We have recently provided direct evidence for such a role by demonstrating that the MT-destabilizing activity of ectopic Op18 is switched off in intact cells by cotransfection of the two distinct cognate kinases, Ca^{2+}/calmodulin–dependent protein IV/Gr

Address correspondence to Martin Gullberg, Department of Cell and Molecular Biology, University of Umeå, S-901 87 Umeå, Sweden. Tel.: 46-90-7852532. Fax: 46-90-771420. E-mail: martin.gullberg@cmb.umu.se

The present address for Bonnie Howell is Department of Biology, University of North Carolina, Chapel Hill, NC 27599.

1. *Abbreviations used in this paper:* AMP-PNP, adenyl-5′-yl imidodiphosphate; GST, glutathione-S-transferase; MT, microtubule; Op18, oncoprotein 18/stathmin.

and cAMP-dependent protein kinase (Gradin et al., 1997, 1998).

Op18 is a prototype member of a new family of proteins with microtubule regulatory function (Ozon et al., 1997; Riederer et al., 1997; Gavet et al., 1998), but the primary sequence does not give any clues to the mechanism involved. Microinjection of neutralizing anti–Op18 antibodies into newt lung cells results in a 2.5-fold increase in MT polymer and an associated decrease in catastrophe frequency, which suggests a physiological importance of Op18 for regulation of the MT system (Howell et al., 1999a). Evidence has been presented that support two different mechanisms for Op18-mediated MT destabilization: (1) simple tubulin sequestration (Curmi et al., 1997; Jourdain et al., 1997) or (2) specific promotion of microtubule catastrophes (Belmont and Mitchison, 1996). In a more recent study (Howell et al., 1999b), which involved in vitro MT assembly assays, we showed that a specific catastrophe promoting activity of Op18 is predominant at physiological pH (~7.4) and that the sequestering activity is predominant at pH 6.8. This was consistent with the reported pH dependence of Op18–tubulin binding (Curmi et al., 1997), since lowering the pH appears to increase the binding affinity. The first indication that Op18 has the potential to destabilize MTs by more than one mechanism came from a mutational analysis in vitro, where it was found that the NH_2-terminal region of Op18 possesses determinants essential for catastrophe promotion, whereas the COOH-terminal region possesses determinants essential for reduced polymerization rate (Howell et al., 1999b). To mechanistically understand Op18 action, we addressed the importance of the stability of the Op18–tubulin complex by analyzing the phenotypes of two classes of mutations (Larsson et al., 1999). One class was mutated in heptad repeats of hydrophobic residues and the other involved substitution of phosphorylation sites to negatively charged glutamic acid residues. Both classes of Op18 mutants were partially compromised in their tubulin binding but the MT-destabilizing activities of the class of mutants with exchange of hydrophobic residues were more severely reduced in intact cells than the glutamic acid–substituted Op18 derivative. Analysis of Op18 activities, such as stimulation of tubulin GTP hydrolysis and inhibition of tubulin polymerization, revealed that the class of mutants with exchange of hydrophobic residues was essentially inactive, whereas the glutamic acid–substituted Op18 derivative was active. This suggested that Op18 transmits tubulin-directed signals that are independent of the stability of the Op18–tubulin complex, and that tubulin sequestering is not of major functional importance.

As outlined above, Op18 lacks any cues or signatures in its primary sequence indicative for a specific mechanism of action. Here, using truncated derivatives of Op18, we have defined distinct region-specific tubulin GTPase-modulating activities and determined how these in vitro activities segregate from tubulin binding properties and specific MT-regulating activities in intact cells. The results provide a clear demonstration that Op18 regulation of MTs in intact cells is independent of tubulin sequestering, and that this regulatory protein is versatile in its tubulin/MT–directed activities and has the potential to regulate MT dynamics by distinct mechanisms.

Materials and Methods

DNA Constructs, Expression and Purification of Recombinant Proteins

Human Op18 derivatives, with or without an 8–amino acid COOH-terminal Flag epitope, were expressed using the pET-3d expression vector and purified from *Escherichia coli* as described (Marklund et al., 1994). The COOH-terminal–truncated Op18, with the sequence encoding amino acids 100–147 deleted (Op18-Δ100-147), and the NH_2-terminal–truncated Op18, with the sequence encoding amino acids 5–55 deleted (Op18-Δ5-55), were constructed using PCR strategies (Marklund et al., 1994). The same strategies were used to construct the Op18-Δ5-9, Op18-Δ5-16, Op18-Δ5-25, Op18-Δ5-38, Op18-Δ5-46, and Op18-Δ90-147 derivatives and primer sequences are available from the authors on request. Constructs for expression of glutathione-S-transferase (GST)–Op18 fusion proteins in *E. coli* were generated by inserting an NcoI-NotI fragment of wild-type and deleted Op18 derivatives into NcoI-EcoRI–digested pGEX 4T-1 (Pharmacia) together with a double stranded adapter of the two oligonucleotides: 5′-AATTCGCGGC-3′ and 5′-CATGGCCGCG-3′. The GST-Op18 fusion proteins were expressed and purified on glutathione-Sepharose 4B beads as recommended by the manufacturer (Pharmacia). For expression of Op18 deletion mutants in human cell lines, Op18 derivatives were excised from pBluescript SK+ using HindIII and BamHI, and Op18 fragments were cloned into the corresponding sites of the EBV-based shuttle vector pMEP4 (Invitrogen Corp.; Marklund et al., 1994).

Assays of Tubulin GTPase Activity

Analysis of tubulin GTPase activity was performed in PEM buffer (80 mM piperazine-*N*,*N*′-bis[2-ethanesulfonic acid], 1 mM EGTA, 4 mM Mg^{2+}, pH 6.8) containing 17% glycerol and 5 mM adenyl-5′-yl imidodiphosphate (AMP-PNP; to inhibit nonspecific ATPase activity).

GTPase activity in the presence of free GTP, which allows multiple substrate turnover, was monitored by incubating tubulin (5–10 μM) with α-[^{32}P]GTP (100 μM; 2×10^6 dpm per 25-μl reaction) at 37°C in the absence or presence of specific Op18 derivatives. To analyze exchange independent GTP hydrolysis in a single turnover reaction, tubulin (100 μM) was preloaded with α-[^{32}P]GTP (100 μM; 50×10^6 dpm per 25-μl reaction) on ice for 30 min. Tubulin in complex with α-[^{32}P]GTP was recovered by centrifugation through a desalting column (P-30 Micro Bio-Spin; Bio-Rad Laboratories) and GTP hydrolysis was followed at 37°C. In the absence of tubulin, but in the presence of BSA or Op18 (15 μM), these columns retained >99.99% of all α-[^{32}P]GTP. Control experiments showed that the Op18 preparations used neither bind nor hydrolyze α-[^{32}P]GTP.

Nucleotide hydrolysis was quantitated as described (Austin and Dixon, 1992). In brief, aliquots were removed at the times indicated, adjusted to contain 0.1% SDS, and heated for 2 min at 80°C. Aliquots (0.6 μl) were spotted onto polyethyleneimine cellulose plates (Merck) and GDP-separated from GTP by ascending chromatography in 1.2 M NH_4COOH acidified with 1.2 M HCl. PhosphorImager (Molecular Dynamics, Inc.) analysis of radioactive spots was used for quantification.

Analysis of Op18–Tubulin Binding

Analyses of Op18–tubulin association in crude extracts from transfected K562 cells were performed after cell lysis (50×10^6 per ml, on ice) in PEM buffer, pH 6.8, containing glycerol (5%), Triton X-100 (0.5%), β-glycerophosphate (10 mM), leupeptin (20 μM), pefablock (1 mM), and benzamide (1 mM). Cell extracts were clarified by centrifugation and, thereafter used for pull-down assays as described below. For equilibrium binding experiments, COOH terminally Flag-tagged wild-type and truncated Op18 derivatives (2–10 μM) and tubulin (0.8–36 μM) were mixed and allowed to associate on ice for ~15 min to ensure equilibrium. Independent of the Op18 derivative tested, association of Op18–F-tubulin complexes is rapid and equilibrium reached within a few minutes (data not shown and Howell et al., 1999b). Op18–Flag-tubulin mixes (48 μl) were added to agarose beads (12 μl) coupled with the Flag-epitope specific M2 antibody (Sigma Chemical Co.), and incubated for 30 min at 8°C to capture Op18-Flag-tubulin complexes. Alternatively, glutathione-Sepharose beads (Pharmacia) were used to analyze tubulin binding to NH_2 terminally GST-tagged Op18 derivatives.

To allow rapid separation of Op18–tubulin complexes bound to M2 or

glutathione beads, the bead suspension was applied into the cap of a 1.5-ml Eppendorf tube containing a bottom layer of 0.4 ml of PEM complemented with 27%:17% sucrose/glycerol, pH 6.8, and a top layer of 0.2 ml of PEM with 17% glycerol, pH 6.8. The caps were closed with care, to keep the bead suspension hanging in the cap, and the samples were centrifuged (for 1 min at 21,000 *g*) to separate bead-bound and free material. The supernatants and pellets were boiled in SDS–sample buffer and resolved by 10–20% gradient SDS-PAGE as described (Brattsand et al., 1993). Tubulin and Op18 content were quantified by Coomassie blue staining of protein bands followed by scanning using a personal densitometer (Molecular Dynamics). Bovine tubulin and a standard recombinant Op18 preparation, in which the protein mass had been determined by amino acid analysis, were used as internal standards. In a more sensitive binding assay, binding was analyzed after labeling of tubulin with α-[^{32}P]GTP as described above under Assays of Tubulin GTPase Activity. Control experiments confirmed that in the absence of free GTP, α-[^{32}P]GTP remained stably associated with tubulin over the time-course of the assay, both in the presence and absence of Op18. A trace of ^{125}I–Op18-F was also included to allow simultaneous quantification of Op18 and tubulin in the same sample. There are two major benefits with this strategy. First, the amount of Op18-F (~30% of total Op18-F) present in the fraction of free tubulin after separation of M2-coupled beads can be compensated for in each data point and, second, only biologically active (i.e., GTP bound) tubulin was detected in the fraction of free tubulin. The contribution of nonspecific tubulin binding was generally ~3% of the amount of free tubulin and was subtracted from presented data. Since the position of the epitope tag used for pull-down of Op18–tubulin complexes may influence binding, in particular if large deletions are introduced close to the epitope tag, tubulin binding of Op18 derivatives was analyzed using either the NH_2-terminal GST-tag or COOH-terminal Flag-tag. The data showed that the position of the epitope tag does not significantly alter Op18–tubulin binding characteristics (data not shown).

To calculate equilibrium dissociation constants, data points from equilibrium binding experiments were fitted either to a hyperbola or to a model assuming two-site positive cooperativity in binding (Koshland et al., 1966). Written in the form of a binding curve, a two-site positive cooperativity model has the form,

$$B = \frac{B\,\max}{2} \times \left\{ 1 / \left[1 + \frac{2F}{K_d1} + \frac{F^2}{(K_d1 \times K_d2)} \right] \right\} \times \frac{2F}{K_d1} \left(1 + \frac{F}{K_d2} \right),$$

where K_d1 and K_d2 are the equilibrium dissociation constants for Op18 binding of the first and second tubulin heterodimer respectively, B is the Op18/tubulin molar ratio of complex-bound proteins, and F is the free tubulin concentration. Comparison of fits was performed using the F-test provided by GraphPad Prism (GraphPad Software, Inc.).

To determine dissociation rates of Op18–tubulin complexes, M2 beads coated with Flag-tagged Op18 derivatives were incubated with tubulin (20 μM) for 15 min at 8°C to attain equilibrium binding. Before centrifugation through a sucrose/glycerol cushion, bead suspension was diluted 100-fold in PEM ± glycerol (17%) and incubated for 20–900 s. Op18–tubulin complexes were quantitated by the dual isotope labeling strategy described above. Dissociation rates were calculated assuming one phase exponential decay using GraphPad Prism software.

SDS-PAGE and Quantitative Western Blotting

Cells were washed in PBS and disrupted by boiling in SDS–sample buffer. The cell extract was clarified by centrifugation and, thereafter, separated by 10–20% gradient SDS-PAGE, followed by transfer to nitrocellulose filters. Cellular Op18 was detected by probing filters with affinity-purified anti-Op18 (Brattsand et al., 1993). For detection of Flag epitope-tagged Op18, the anti–Flag-M2 antibody (Sigma Chemical Co.) was used. Cellular tubulin was detected by probing filters with anti–α-tubulin (clone B-5-1-2; Sigma Chemical Co.). Probing of filters, detection of specific antibodies by ^{125}I–protein A, and PhosphorImager analysis of radioactive bands was performed as described (Brattsand et al., 1993). Quantification of Op18 and tubulin in cell lysates was obtained by comparing signals with standard curve generated by separating graded amounts of bovine tubulin and recombinant Op18 on the same SDS-PAGE. The errors between independent determinations were routinely <20% and the protein mass of bovine tubulin and recombinant Op18 was determined by amino acid analysis.

Transfection of Human K562 Erythroleukemia Cells, Analysis of MT-polymerization Status, and Flow Cytometric Analysis

The conditions used for transfection studies and the pMEP4 shuttle vector system have been described previously (Marklund et al., 1994). Conditional expression of various Op18 derivatives was achieved by using the hMTIIa promoter, which can be suppressed by low concentrations of EDTA (50 μM) and induced by Cd^{2+} (0.5 μM; Marklund et al., 1994). The amount of pMEP-Op18 constructs per electroporation was adjusted to obtain comparable expression levels of all Op18 derivatives. 5 μg DNA was used of pMEP-Op18-wt-F and pMEP-Op18-Δ5-9-F, whereas 12.5 μg was used of pMEP-Op18-Δ5-25-F and Op18-Δ100-147-F.

The cellular content of MT polymers was determined by extracting soluble tubulin in an MT-stabilizing buffer followed by quantification of tubulin in the particulate and soluble fraction as described (Minotti et al., 1991; Marklund et al., 1996). For flow cytometric analysis, cells were extracted, fixed, and stained with anti–α-tubulin (clone B-5-1-2) as described (Gradin et al., 1998). Analysis of 150,000 cells per transfected Op18 derivative was performed using a FACs-calibur together with the Cell Quest software (Becton Dickinson & Co.).

Culture and Microinjection Studies on Primary Newt Lung Epithelial Cells

Primary cultures of newt lung cells were grown on coverslips in chambers at room temperature (23°C) as previously described (Rieder and Hard, 1990; Howell et al., 1997). For microinjection studies, cells were typically used 4–6 d after each culture had begun. Newt lung cells at the peripheral regions of the cell sheet were microinjected with various Op18 protein derivatives in a 2-mM phosphate buffer. Injected volumes are likely consistent with previous estimates of 5–10% of cell volume (Graessmann et al., 1980; Saxton et al., 1984), resulting in final intracellular concentrations of 8–16 μM of various Op18 derivatives. Cells were injected on an Olympus CK2 inverted microscope with attached Narishige MN-151 manipulator, using a capillary holder and prepulled glass microtips (ID 0.5 μm; World Precision Instruments, Inc.). Cells were microinjected, incubated for 3 h at room temperature, and then lysed and fixed for antitubulin immunofluorescence as described (Howell et al., 1997). Microinjected cells were identified based on their position relative to the tissue explant. Cells were examined using a 60× 1.4 NA Plan Apo objective on an Olympus BH-2 microscope. Images were projected to an MTI CCD-72 camera, integrated (32 frames), and stored using NIH Image software (version 1.57). The final figure was composed using Canvas 6.0 software (Deneba Software).

Results

Molecular Dissection of Distinct Tubulin GTPase-modulating Activities of Op18

Complex formation with tubulin is a likely minimal requirement for tubulin-directed signals of Op18. To analyze tubulin complex formation of the series of NH_2- and COOH-terminal truncations of Op18 depicted in Fig. 1 A, Flag epitope-tagged Op18 (Op18-F) and tubulin were mixed at an equimolar ratio (10 μM each). Op18-F-tubulin complexes were recovered using anti–Flag antibody coupled beads together with a rapid one-step gradient protocol. The bead-bound Op18-F-tubulin complexes were resolved and quantified by SDS-PAGE followed by densitometric scanning of stained gels. The result shows that at a 1:1 molar ratio, essentially all tubulin was in complex with Op18-wt (Fig. 1 B). A partial loss of tubulin binding was evident after truncations of the NH_2-terminal region covering amino acids 5–9 to amino acids 5–46. Further truncation into the functionally important heptad repeats (Op18-Δ5-55; Larsson et al., 1999) results in a major loss of tubulin binding. It is also shown that large COOH-terminal truncations, represented by the Op18-Δ100-147 and

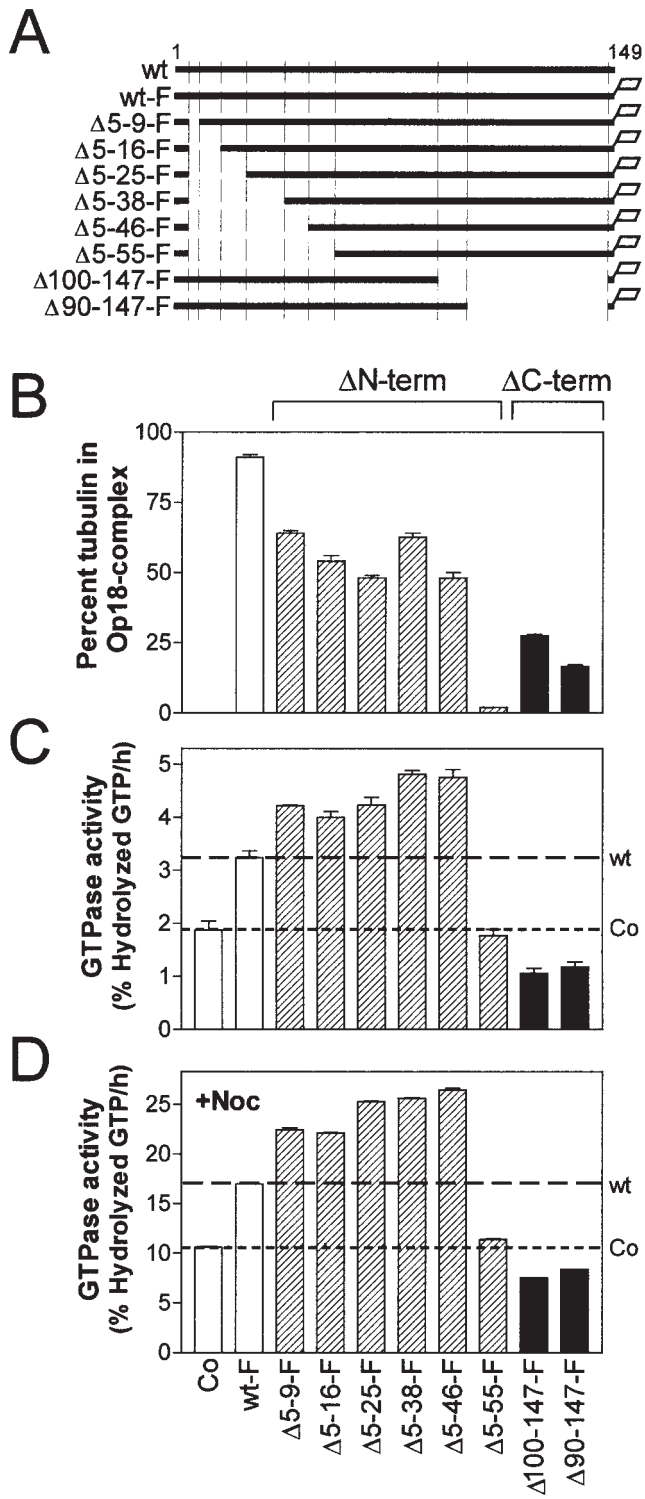

Figure 1. Tubulin binding and modulation of tubulin GTPase activity by Op18 deletion mutants reveal region specific tubulin-directed activities. (A) Schematic representation of Flag-tagged deletion derivatives of Op18. (B) Tubulin binding to the indicated Op18 Flag-epitope–tagged derivatives was analyzed at equimolar concentration (10 μM) in PEM, pH 6.8, containing 17% glycerol. The Op18–tubulin mixture was incubated at 37°C together with anti-Flag coated beads for 30 min and bead-bound material was pelleted through a sucrose/glycerol cushion. The percent of the tubulin recovered in complex with Op18 was determined by densitometric scanning of Coomassie blue–stained SDS-PAGE gels. (C and D) Tubulin (10 μM) GTPase activity was determined in the presence of the indicated Op18 derivatives (15 μM). Samples were incubated at 37°C for 90 min with α-[^{32}P]GTP (100 μM) in PEM, pH 6.8, containing 17% glycerol in the absence (C) or presence (D) of nocodazole (33 μM). To facilitate comparison, GTPase activity in the absence (Co) or presence of Op18-wt-F (wt) are indicated by dashed lines. The means of duplicate determinations of hydrolyzed GTP are shown and data are representative for at least three independent experiments.

Δ90-147 derivatives, result in a major loss of tubulin binding.

The next step in the analysis was to determine the effect of Op18 truncations on stimulation of tubulin GTPase activity. This analysis was performed under identical buffer conditions and tubulin concentrations as in Fig 1 B. Under these conditions, Op18-wt causes a modest 1.7-fold increase in the basal tubulin GTPase activity (Fig. 1 C). Interestingly, despite decreased tubulin binding, truncations in the NH_2-terminal region up to amino acid 46 result in enhanced GTPase activity. Decreased tubulin binding of the COOH-terminal–truncated derivatives was associated with the opposite activity, namely significant suppression of the basal tubulin GTPase activity. Consistent with its lack of tubulin binding, Op18-Δ5-55 showed no detectable modulation of GTPase activity.

Fig. 1 D shows Op18-mediated stimulation of tubulin GTPase activity in the presence of nocodazole, an MT-disrupting agent that by itself stimulates tubulin GTPase activity. Nocodazole, under these conditions, mediates a fivefold enhancement of both basal and Op18-wt–stimulated GTPase activity. Interestingly, albeit that there is a general fivefold increase, we observed the same pattern of GTPase stimulatory/suppressive activities of the truncated Op18 derivatives as in the absence of nocodazole. Since truncations of an NH_2-terminal region of Op18 results in enhanced stimulation of tubulin GTPase activity, and truncation of a COOH-terminal region results in suppression of both the basal- and nocodazole-induced GTPase activity, it appears that the native Op18 contains tubulin binding determinants with multiple regulatory effects on tubulin GTP metabolism.

In the experiments shown in Fig. 1, the tubulin concentration is too low to support detectable polymerization (data not shown). In the assays performed in the presence of the antipolymerizing drug nocodazole, it is even less likely that the observed Op18-specific effects are caused by a mechanism involving tubulin polymerization. Furthermore, all the Op18 derivatives tested, except Op18-Δ5-55, mediate varying degrees of antipolymerizing activity under the present conditions (data not shown). Hence, we conclude that the activity profiles of the truncated Op18 derivatives reflect modulation of the tubulin GTPase activity under nonassembly conditions.

Op18 may modulate tubulin GTP metabolism by altering the rate of nucleotide exchange and/or hydrolysis. To specifically analyze Op18 regulation of the GTP hydrolysis rate, selected Op18 derivatives were mixed in the presence of nocodazole with tubulin prebound to α-[^{32}P]GTP (note that a threefold molar excess of Op18 was used to increase the fraction of tubulin in complex with mutated Op18). The assay was performed in the absence of free GTP, and

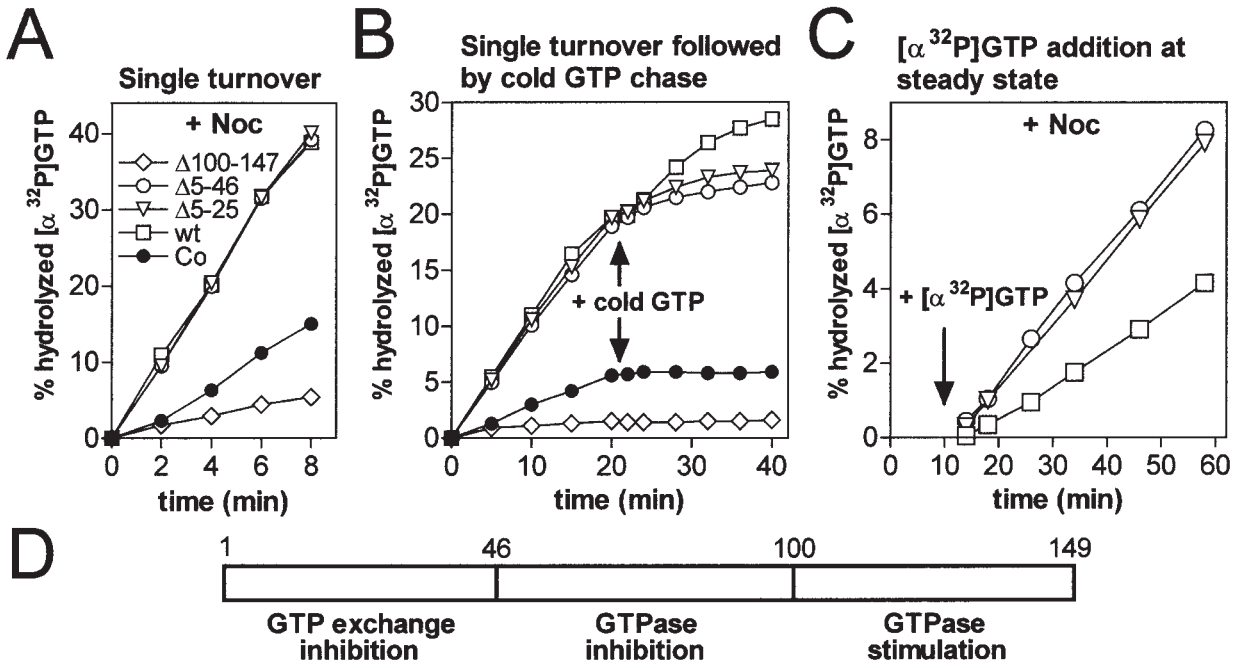

Figure 2. Independent regions of Op18 regulate the rate of tubulin GTP hydrolysis and nucleotide exchange. (A) Modulation of tubulin (5 μM, in PEM with 17% glycerol, pH 6.8) GTP hydrolysis rates were determined in the presence of the indicated Op18 derivatives (15 μM). Hydrolysis of α-[^{32}P]GTP preloaded onto tubulin (i.e., a single turnover event) was followed over time in the presence of nocodazole (33 μM). (B) Modulation of tubulin GTP hydrolysis rates in the absence of nocodazole was followed for 20 min with different Op18 derivatives (conditions and symbols as in A). After 21 min, the reaction was chased by addition of 200 μM of cold GTP and the effect on hydrolysis of α-[^{32}P]GTP was followed over time. (C) GTP exchange dependent α-[^{32}P]GTP hydrolysis was analyzed by mixing tubulin (5 μM, buffer as in A and B and 33 μM nocodazole) with the indicated Op18 derivatives (15 μM, same symbols as in A) and unlabeled GTP (100 μM). After 10 min at 37°C, α-[^{32}P]GTP was added to the reaction mixtures and GTP hydrolysis was followed over time. The means of duplicate determinations are shown. (D) A schematic representation of the importance of distinct Op18 regions for modulation of tubulin GTP metabolism.

hydrolysis of tubulin-bound α-[^{32}P]GTP (i.e., a single turnover event) was followed over time. As shown in Fig. 2 A, in contrast to the result obtained in the presence of free α-[^{32}P]GTP in the reaction mix (Fig. 1 D), the data show that Op18-wt and NH_2-terminal–truncated derivatives were indistinguishable in their stimulation of GTP hydrolysis in a single turnover assay. It is also shown that the COOH-terminal–truncated derivative (Δ100-147) has a potent suppressive effect on the rate of GTP hydrolysis. Since nocodazole was included in the reaction mix, which results in a fivefold increase in both the basal- and Op18-stimulated level of GTP hydrolysis (Fig. 1), it appears that this derivative exerts a general suppression of tubulin GTP hydrolysis.

In the presence of free α-[^{32}P]GTP in the reaction mix, which allows multiple turnovers of GTP, truncation of the NH_2-terminal region of Op18 enhances stimulation of tubulin GTPase activity both in the absence and presence of nocodazole (Fig. 1, C and D). However, in a single turnover reaction, these same derivatives were indistinguishable from Op18-wt (Fig. 2 A). This suggests that Op18-wt may contain an NH_2-terminal region that inhibits GTP exchange. To address this, selected Op18 derivatives and prebound α-[^{32}P]GTP-tubulin were first mixed, and GTP hydrolysis in the absence of nocodazole was followed for 20 min at 37°C. As shown in Fig. 2 B, Op18-wt and NH_2-terminal–truncated derivatives show the same stimulation of tubulin α-[^{32}P]GTP hydrolysis, as measured in a single turnover assay, whereas the COOH-terminal–truncated derivative suppresses the basal hydrolysis obtained with tubulin alone, which agrees with the data obtained in the presence of nocodazole (Fig. 2 A). To assess if Op18 blocks GTP exchange, the reaction was chased with cold GTP after 21 min and subsequent alterations in the rate of α-[^{32}P]GTP hydrolysis were monitored (Fig. 2 B). As expected from the rapid GTP exchange rate of free tubulin (Brylawski and Caplow, 1983), the data show that a chase with cold GTP results in an immediate attenuation of the basal α-[^{32}P]GTP hydrolysis. In the presence of Op18-wt, however, the result of a chase with cold GTP was modest and the rate of α-[^{32}P]GTP hydrolysis shows only a slow decline with time, which is contrasted by a more profound effect of the chase in the presence of NH_2-terminal–truncated derivatives. This indicates that Op18 exerts a potent tubulin GTP exchange inhibitory activity that involves the NH_2-terminal region.

To further address the importance of the NH_2-terminal region for regulating GTP exchange of tubulin, tubulin and cold GTP were mixed and allowed to reach steady state GTP hydrolysis at 37°C. Thereafter, α-[^{32}P]GTP was added and the generation of α-[^{32}P]GDP was monitored. This protocol provides selective detection of GTP hydrolysis after exchange to a labeled nucleotide. Given the indistinguishable GTP hydrolysis rates in the presence of wt and NH_2-terminal–truncated derivatives (Fig. 2, A and B),

inhibition of nucleotide exchange would be manifested as decreased generation of α-[^{32}P]GDP in the presence of Op18-wt. As predicted, the data in Fig. 2 C shows that NH_2-terminal truncation of Op18 results in a twofold increase of α-[^{32}P]GTP hydrolysis as compared with the native Op18 protein. Thus, Op18-mediated inhibition of GTP exchange via its NH_2-terminal region provides a mechanism that explains the observation that NH_2-terminal truncation enhances stimulation of tubulin GTPase activity under conditions allowing multiple turnovers of GTP (Fig. 1, C and D).

Inhibition of GTP exchange together with the demonstrated positive and negative modulation of the rate of GTP hydrolysis, as schematically outlined in Fig. 2 D, indicates that Op18 binding to tubulin results in multiple tubulin-directed activities that can be genetically dissected and assigned to specific regions of the protein. Since the COOH-terminal is essential for stimulating hydrolysis, whereas deletion of this region results in a derivative with the opposite activity, namely suppression of the GTP hydrolysis rate, it appears that there exist regions in the remaining polypeptide that must counteract the stimulatory activity of the COOH-terminal. Since Op18-Δ5-46 stimulates GTP hydrolysis to the same extent as Op18-wt, it follows that the region with suppressive potential would be located between amino acids 46 and 100 as depicted in Fig. 2 D. However, it is not possible to test this prediction by deletion analysis since Op18-Δ5-46 represent the largest possible NH_2-terminal truncation that does not cause termination of tubulin binding and, thereby, modulation of GTPase activity (Fig. 1, see Op18-Δ5-55).

Op18 and Tubulin Form Dynamic Complexes

It has been proposed that the Op18–tubulin complex is relatively stable since it resists gel filtration and analytical ultracentrifugation (Curmi et al., 1997; Jourdain et al., 1997). To evaluate if the tubulin-directed activities described above is the result of a stable complex between Op18–tubulin or, alternatively, if Op18 mediates tubulin-directed activities in a dynamic complex, we determined the dissociation rates of selected Op18 derivatives in the presence or absence of glycerol as described in Materials and Methods. The data in Table I show that Op18-wt-tubulin complexes have a rapid dissociation rate that decreases about fourfold in the presence of glycerol. The dissociation rate constant in the absence of glycerol (0.010 s^{-1}) is similar to what has been reported using plasmon resonance measurement (0.005 s^{-1}; Curmi et al., 1997). NH_2-terminal truncations result in faster dissociation that is slowed down ~10-fold by glycerol. The Op18-Δ100-147 derivative formed the most unstable complex with tubulin and glycerol has only a minor stabilizing effect. In conclusion, Op18 forms dynamic complexes with tubulin and, in the case of Op18-Δ100-147, the complex has a half-life of ~35 s in the buffer conditions used throughout this study (i.e., in the presence of glycerol).This indicates that Op18 modulates GTP hydrolysis by multiple transient tubulin interactions during the time of the assay and not by forming stable complexes with tubulin.

The dynamic nature of the Op18–tubulin complex may appear contradictory to a previous report by us in which we employed a similar experimental approach (Larsson et al., 1999). Thus, we noted that the estimated Op18/tubulin ratio was ~1:3 at equilibrium, and upon a 20-fold dilution the ratio rapidly changed to an apparently stable 1:2 ratio. Therefore, we suggested that one Op18 complexed with three tubulins rapidly changed upon dilution to a stable complex containing two tubulins. However, the apparent stability was due to formation of a new equilibrium after the dilution step. This misinterpretation, together with a 33% error in our previous estimation of Op18/tubulin molar ratio, was the cause of this misconception.

Table I. Op 18–Tubulin Complexes Are Dynamic

	Glycerol	± SE	$T_{1/2}$ ± SE
		(s^{-1})	(s)
Op18-wt-F	0%	0.010 ± 0.0007	70 ± 5.1
Op18-Δ5-25-F	0%	0.022 ± 0.0009	32 ± 1.4
Op18-Δ5-46-F	0%	0.022 ± 0.0014	31 ± 1.9
Op18-Δ100-147-F	0%	0.036 ± 0.0024	19 ± 1.2
Op18-wt-F	17%	0.0025 ± 0.0009	274 ± 98
Op18-Δ5-25-F	17%	0.0021 ± 0.0004	324 ± 67
Op18-Δ5-46-F	17%	0.0022 ± 0.0003	311 ± 41
Op18-Δ100-147-F	17%	0.020 ± 0.0019	35 ± 3.3

Determination of dissociation rates, expressed as either k (s^{-1}) or half-lives ($T_{1/2}$, s) of Op18–tubulin complexes was determined in the absence and presence of 17% glycerol, assuming one phase exponential decay as described in Materials and Methods.

Op18 Binds Two Tubulin Heterodimers Via Multiple Regions by a Mechanism Involving Two-site Positive Cooperativity

As shown above, Op18 deletion mutants are useful analytical tools to dissect modulation of tubulin GTP metabolism, and the results suggest that physically separate tubulin binding motifs of Op18 transmit distinct tubulin-directed signals. Assuming that separate tubulin binding motifs are all involved in the overall binding affinity between Op18 and tubulin, specific truncations would be anticipated to result in a step-wise loss of affinity. To approach these questions, we performed detailed analyses of Op18–tubulin interactions. Op18–tubulin association previously has been shown to be rapid, and equilibrium is reached in <5 min using either wild-type (Curmi et al., 1997) or truncated derivatives (Howell et al., 1999b). Selected COOH terminally Flag-tagged Op18 derivatives, and their NH_2 terminally GST-tagged counterparts (see Materials and Methods) were analyzed for their ability to bind tubulin over a range of concentrations by the strategy described under Fig. 1. Scatchard analysis of these data showed that all Op18 derivatives tested, bind close to 2 mol tubulin per mol (Op18-wt, 2.3 ± 0.07; Op18-Δ5-9, 2.1 ± 0.05; Op18-Δ5-25, 2.1 ± 0.08; and Op18-Δ100-147, 2.0 ± 1.3; three independent determinations in PEM, pH 6.8). However, because of difficulties to quantify low tubulin concentrations by scanning Coomassie blue–stained gels, the independence or cooperativity in Op18–tubulin binding was difficult to assess. Therefore, we adopted a strategy involving labeling of tubulin with α-[^{32}P]GTP. Control experiments showed that in the absence of free GTP, α-[^{32}P]GTP remained stably associated with tubulin over

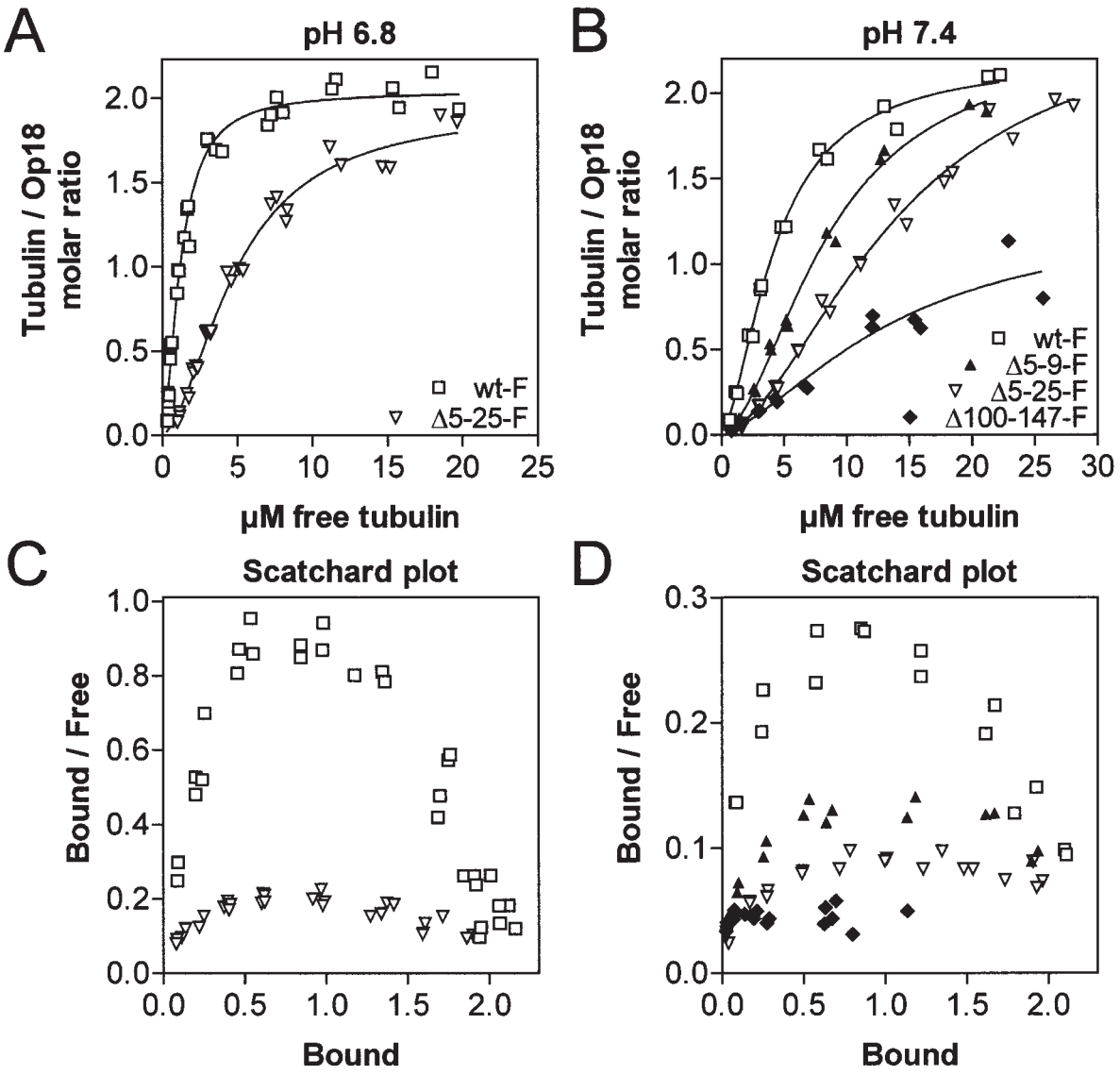

Figure 3. Complexes between Op18 and two tubulin heterodimers are generated via two-site positive cooperativity. Op18–tubulin equilibrium binding curves at pH 6.8 (A) and 7.4 (B) were determined for the indicated Op18 derivatives (2 mM) at 8°C as described in Materials and Methods. The contribution of nonspecific binding (3% of free tubulin) is subtracted. Curves assuming two-site positive cooperative binding were fitted to the data points. Scatchard conversion of the binding curves are shown below (note difference in scales in C and D). Data are representative for two independent experiments.

the time-course of the assay both in the presence and absence of Op18 (for 30 min at 8°C). To allow simultaneous quantification of Op18 and tubulin in the same sample, a trace of ^{125}I-Op18-F was added. Using this dual labeling approach, we obtained bindings curves of sufficient quality for detailed analysis of affinities (Fig. 3). It is clear from the binding curves for Op18-wt that half saturation of tubulin binding to Op18-wt is reached at 1.2 μM at pH 6.8 (A) and 4.3 μM at pH 7.4 (B). A previous study has also noted pH regulation of affinity (Curmi et al., 1997), and, in this study, an equilibrium dissociation constant (K_d) of 0.5 μM at pH 6.5 was determined by plasmon resonance measurement, which is in reasonable agreement with our data obtained at pH 6.8. However, Scatchard analysis of both pHs (C and D), shows that tubulin binding to Op18 is a complex process with observed nonlinear data point distribution typical for positive cooperativity in binding (Koshland et al., 1966). Analysis of tubulin binding curves of selected Op18 mutants showed that half saturation of NH_2-terminal truncation derivatives requires two to fourfold higher tubulin concentrations, as compared with Op18-wt, and that the COOH terminally truncated protein is most severely affected in its tubulin affinity. Since the position of the epitope tag used for pull-down may influence the effect of specific truncations, we also analyzed tubulin binding of selected Op18 derivatives tagged in the NH_2 terminus with GST (see Materials and Methods). The results obtained using GST-tagged derivatives were essentially the same as using the COOH-terminal Flag-tag (data not shown). Hence, the binding appears independent of

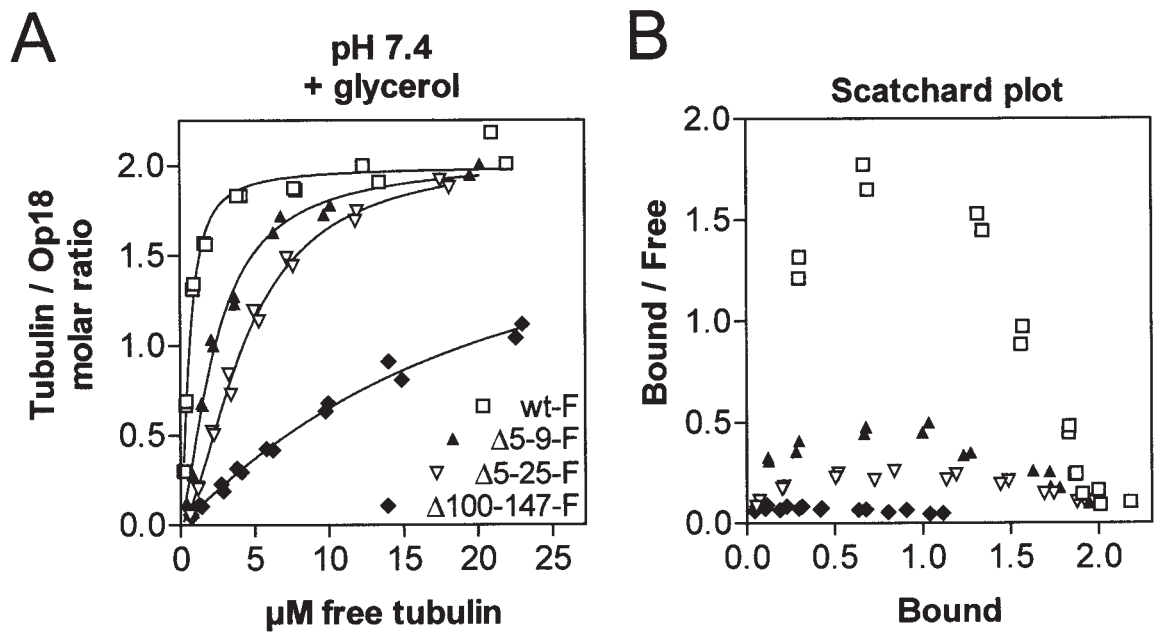

Figure 4. Glycerol increases Op18–tubulin binding affinity in accordance with a two-site positive cooperativity model. (A) Op18–tubulin equilibrium binding curves using the indicated Op18 derivatives (2 μM) was determined in the presence of 17% glycerol as in Fig. 3. Scatchard conversions of binding curves are shown in (B).

the position of the epitope tag. It is notable that tubulin binding to all Op18 derivatives tested is a cooperative process as indicated by the sigmoidal binding curves and nonlinear Scatchard plots.

Glycerol, which is commonly used in tubulin buffers, slows down Op18–tubulin dissociation (Table I). In agreement with this result, it is shown in Fig. 4 A that glycerol enhances tubulin binding of Op18-wt and NH_2 terminally truncated derivatives. The binding of Op18-Δ100-147 was essentially unaltered, consistent with the minor effect of glycerol observed on the dissociation rate of this derivative. The experiment in Fig. 4 was performed with 17% glycerol, but even 6% glycerol was sufficient for a major enhancement in tubulin binding (data not shown). The presence of glycerol shifts the curves of the nonlinear Scatchard plots but the data are still typical for positive cooperativity in the interaction.

Two-site positive cooperativity implies that Op18 first binds one tubulin with a given affinity (termed K_d1), and this generates a second site with a higher affinity (termed K_d2). A two-site positive cooperativity model gives the best fit with experimental data, obtained using different buffer conditions in Figs. 3 and 4, and was used to calculate K_d1 and K_d2. The results are summarized in Table II. Deletion analysis shows that both the NH_2- and COOH-terminal regions are important for binding of the first tubulin (defined by K_d1), and this is particularly evident in the presence of glycerol, which primarily enhances K_d1. It is also clear that COOH-terminal truncation, as defined by Op18-Δ100-147, results in a major decrease in binding of the second tubulin (defined by K_d2), whereas NH_2-terminal truncations have only a minor effect. Finally, comparison of Op18-wt with deletion mutants reveals a stepwise decrease in affinity as reflected by K_d1 and K_d2 as well as the estimated free tubulin concentration required for half saturation of Op18. This indicates that Op18 binds tubulin via multiple nonessential contact points distributed over a major part of the Op18 sequence. This is consistent with the above dissection of tubulin-directed activities of Op18, which reveals multiple tubulin-directed activities that can be separated by deletion analysis and assigned to distinct regions spanning a major part of the Op18 peptide. Hence, the data support a model where physically separate tubulin binding motifs of Op18 transmit distinct tubulin-directed signals.

Table II. Calculations According to a Two-site Positive Cooperativity Model Reveal Dependency of Tubulin Binding Affinities on Specific Op18 Regions

	pH	Glycerol	K_d1 ± SE	K_d2 ± SE	Free [tubulin] at half saturation of Op18
			μM	*μM*	*μM*
Op18-wt-F	6.8	0%	7.5 ± 2.9	0.20 ± 0.09	1.2
Op18-Δ5-25-F	6.8	0%	36 ± 17	0.68 ± 0.40	5.0
Op18-wt-F	7.4	0%	19 ± 5.4	1.0 ± 0.38	4.3
Op18-Δ5-9-F	7.4	0%	74 ± 37	0.98 ± 0.60	7.1
Op18-Δ5-25-F	7.4	0%	110 ± 55	1.7 ± 1.1	14.0
Op18-Δ100-147-F	7.4	0%	41 ± 11	16 ± 6.4	25.5
Op18-wt-F	7.4	17%	2.1 ± 0.7	0.19 ± 0.08	0.6
Op18-Δ5-9-F	7.4	17%	6.5 ± 1.4	0.91 ± 0.27	2.4
Op18-Δ5-25-F	7.4	17%	24 ± 7.7	0.82 ± 0.33	4.5
Op18-Δ100-147-F	7.4	17%	24 ± 1.9	15 ± 1.8	19.4

Calculation of equilibrium dissociation constants based on the data shown in Figs. 3 and 4. The free tubulin concentration at half saturation was estimated from curves fitted according to a two-site cooperativity model.

Table III. Intracellular Concentrations of Endogenous/ectopic Op18 and Tubulin in Transfected K562 Cells

	Percentage of total protein* ± SD	Cellular concentration‡ ± SD
		μm
Endogenous tubulin	2.9 ± 0.5%	23 ± 4.2
Endogenous Op18	0.22 ± 0.03%	10 ± 1.4
Op18-wt-F	1.0%	47
Op18-Δ5-9-F	1.4%	65
Op18-Δ5-25-F	1.5%	79
Op18-Δ100-147-F	1.2%	75

*Determination of Op18 and tubulin concentrations after 6 h of induced expression was performed by quantitative Western blot analysis as described in Materials and Methods. ‡Total cytosolic protein concentration was calculated to 80 mg/ml. This is a minimal estimate since the calculation was based on volumes of packed cell pellets.

Op18 Deletion Mutants Fail to Form Complexes with Tubulin in Crude Extracts of Transfected K562 Cells

The significance of Op18 mutant phenotypes observed in vitro was evaluated by transfection experiments using a shuttle vector directing inducible expression of Op18-wt and the deletion derivatives (Marklund et al., 1994). The amount of transfected DNA was adjusted to obtain comparable expression levels of the ectopic proteins in the human K562 cell line. Estimated levels of endogenous tubulin and Op18, together with the induced level of each of the ectopic Op18 derivatives, are shown in Table III. The estimated tubulin concentration (23 μM) is similar to that reported for frog extracts (20 μM; Gard and Kirschner, 1987), and assuming that each Op18 binds two tubulin heterodimers, it is notable that the molar concentration of endogenous Op18 (10 μM) is sufficient for complex formation with essentially all cellular tubulin, even under conditions of complete tubulin depolymerization.

Since Op18-wt has higher affinity for tubulin than the truncated protein, it seems likely that endogenous Op18 levels are sufficient to outcompete tubulin binding of overexpressed deletion derivatives. To test this prediction, we performed an in vitro experiment using components at a similar molar ratio as observed in intact cells. As shown in Fig. 5 A, pull-down assays using GST-fused Op18-wt in the presence of a fivefold molar excess of the indicated Op18 derivatives show the expected 80% competition of tubulin binding by Op18-wt, whereas Op18-Δ5-25 competes with only 20% of the binding and competition by Op18-Δ100-147 is essentially undetectable. In light of this finding, it seems likely that endogenous Op18 will inhibit most of the complex formation of ectopic Op18 deletion mutants with cellular tubulin in transfected cells. This was evaluated in crude cell extracts of K562 cells transfected with Flag-epitope–tagged Op18 (treated exactly as the cells analyzed in Table III). Complex formation was evaluated and as shown in Fig. 5 B, about half of all cellular tubulin is in complex with Op18-wt-F. As predicted, tubulin complex formation by truncated derivatives was much lower. This data predict that the modest five to eightfold overexpression of Op18 deletion mutants would not result in significant tubulin sequestering, and that potential MT destabilization is likely to be attributable to more specific mechanisms.

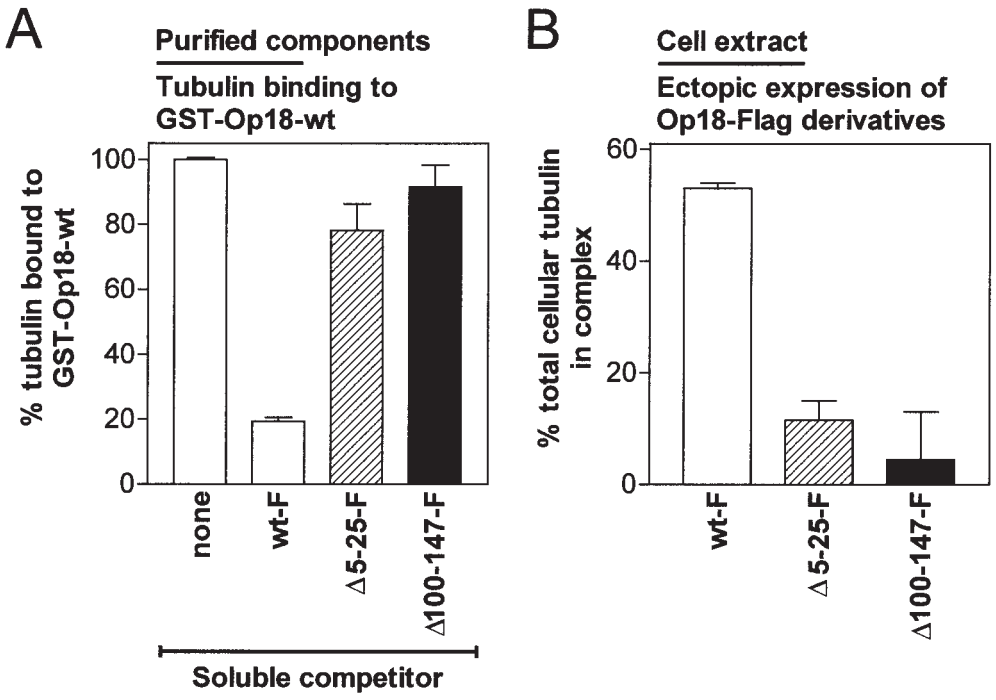

Figure 5. Truncated Op18 proteins fail to compete with Op18-wt for tubulin complex formation. (A) The indicated Op18 derivatives (20 μM) were mixed with bovine tubulin (10 μM) and, thereafter, transferred to pelleted glutathione beads coated with GST-Op18-wt (amount corresponding to 4 μM in the final mixture). After 20 min at 37°C, beads were separated and the GST-Op18/tubulin ratio in complexes was determined as in Fig. 1. The means of three independent experiments are shown. (B) Complex formation between endogenous tubulin and Flag-tagged Op18 was analyzed in extracts of K562 cells induced for 6 h to express the indicated Op18 derivatives. Cell extracts (8 mg of protein/ml) were added to anti-Flag–coupled beads within 10 min of cell lysis (PEM, pH 6.8, 5% glycerol and 0.5% Triton X-100) and incubated for 15 min at 8°C. Bead-bound and soluble material was separated as in Fig. 1 and Op18–tubulin was quantified by Western blot as in Table III. The means of duplicate determinations are shown.

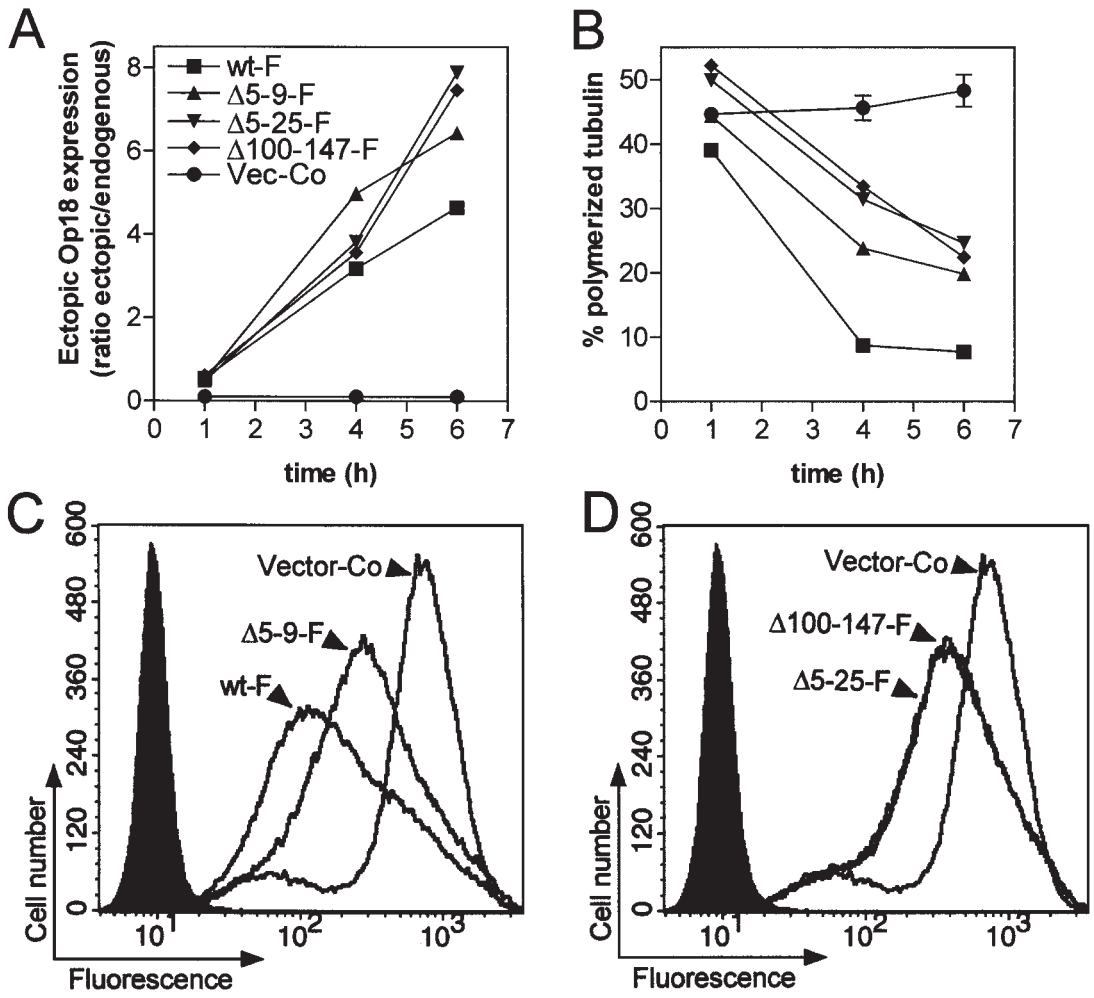

Figure 6. Expression of truncated Op18 proteins destabilize MTs in K562 cells. K562 cells were transfected with the pMEP4 shuttle vector without (Vec-Co) or with insertion of the indicated Op18 derivatives. Transfected cell lines were selected during 5 d in hygromycin and expression from the hMTIIa promoter was induced as described in Materials and Methods. (A) Op18 expression levels, expressed as fold induction over the endogenous Op18 level determined as in Table III. (B) The level of polymerized tubulin, as determined by Western blot analysis of the soluble and particulate fraction of lysed cells. (C and D) Flow cytometric analysis of MTs in the same cell populations shown in A and B (induced to express Op18 for 4.5 h). Open graphs show α-tubulin–specific fluorescence and filled graphs show control staining in the absence of anti–α-tubulin but in the presence of fluorescein-conjugated rabbit anti–mouse immunoglobulin. Histograms depicting control staining and cells expressing vector control are shown in both panels. Median fluorescence signals: control staining, 9; vector control, 698; Op18-wt-F, 168; Op18-Δ5-9-F, 286; Op18-Δ5-25-F, 382; and Op18-Δ100-147-F, 385. Data are representative for at least two independent experiments.

Op18 Mutants Destabilize MTs by a Nontubulin Sequestering Mechanism in Transfected K562 Cells

To search for a phenotype of Op18 deletion mutants, transfected K562 cells were induced to express wild-type and truncated Op18 derivatives for 4 and 6 h. As shown in Fig. 6 A, all the Op18 derivatives analyzed are expressed at comparable levels, and expression of all derivatives results in dramatic MT destabilization (Fig. 6, B–D). Thus, as shown by both biochemical determination (B) and flow cytometric analysis (C and D, note the log scale), all the truncated Op18 derivatives retain at least 50% of wild-type MT destabilizing activity. The specificity of destabilization by the deletion mutants analyzed in Fig. 6 is indicated by previous studies of Op18-Δ5-55, which by several criteria is functionally inactive in vivo (Larsson et al., 1995; Marklund et al., 1996). Since truncated Op18 proteins in the presence of endogenous Op18 have only a minor potential to complex with cellular tubulin (Fig. 5), formation of stable tubulin sequestering complexes cannot explain the phenotype. Hence, Op18 mutants destabilize MTs by more specific mechanisms, possibly involving tubulin/MT–directed signaling.

Fig. 6 shows that both the NH_2-and COOH-terminal–truncated derivatives have a similar gross phenotype with respect to the MT-destabilizing activities, whereas the in vitro analysis shows that these two classes of deletion derivatives have opposite effects on the rates of tubulin GTP hydrolysis. Assuming that the tubulin-directed activities are linked to the phenotype mediated by Op18 derivatives in intact cells, it follows that the NH_2- and COOH-termi-

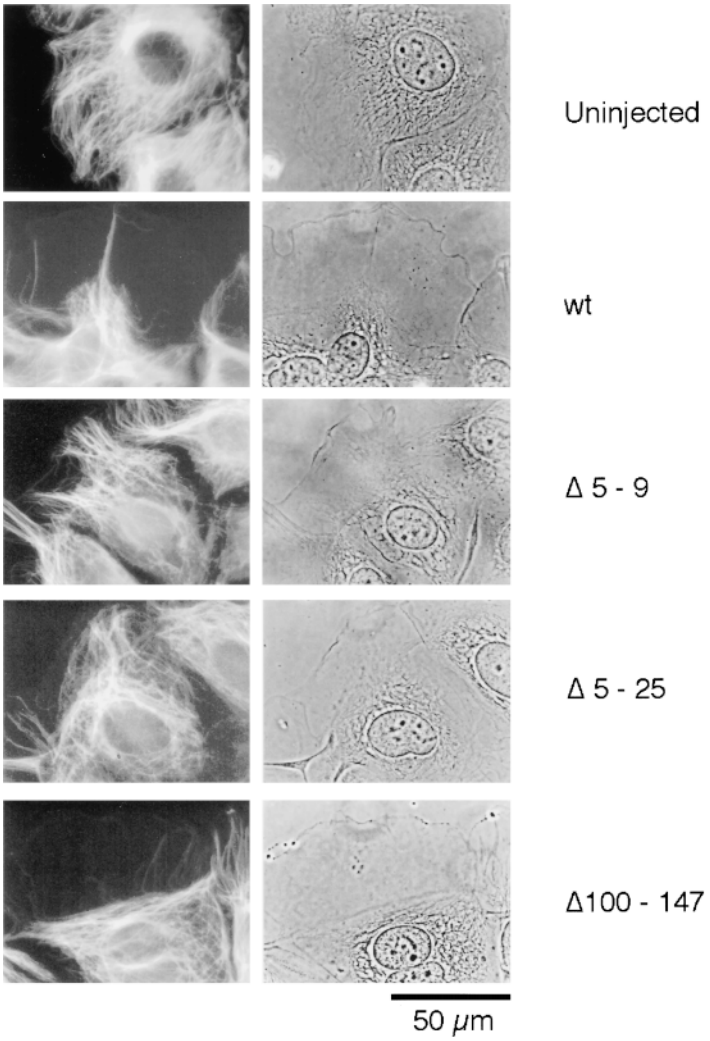

Figure 7. MT appearance in newt lung cells microinjected with low concentrations of Op18 reveal a lamellar clearing phenotype that requires the NH_2-terminal region. Cells were microinjected with the indicated Op18 protein derivative (160 μM needle concentration, 8–16 μM estimated intracellular concentration), fixed, and stained with antitubulin after 3 h, and the MT-network was observed by epi-immunofluorescence. Microinjection of all Op18 derivatives resulted in some loss of MT polymer, but the results from Op18-wt or Op18-Δ100-147 were most pronounced where the lamella regions often lacked MTs, most likely because of MT shortening. Two independent preparations of the recombinant Op18 proteins, expressed with or without the Flag-tag, were used with similar results in microinjection experiments. In the data shown, Op18 proteins without the Flag-tag were used.

nal–truncated mutants cause the same gross phenotype by distinct mechanisms.

Evidence for Distinct MT-directed Activities of Op18 in Intact Cells

A prediction from the proposition above, namely that NH_2- and COOH-terminal–truncated mutants cause MT destabilization by distinct mechanisms, is that the remaining cellular MT networks would exhibit morphological cues, reflecting the different modes of action. The spherical shape of K562 leukemia cells make them unsuitable for morphological analysis. Therefore, we analyzed MTs in newt lung cells 3 h after microinjection of purified Op18 protein derivatives. At high intracellular concentrations (40–100 μM), Op18-wt, Op18-Δ5-9, Op18-Δ5-25, and Op18-Δ100-147 all mediated a massive loss of MT polymer, whereas the inactive variant Op18-Δ5-55 (Marklund et al., 1996) did not alter MT polymers, demonstrating the specificity of Op18-mediated polymer loss (data not shown). To analyze the phenotypes at concentrations similar to that of endogenous Op18 in K562 cells (Table III), Op18 derivatives were microinjected to an estimated intracellular concentration of 8–16 μM. Under these conditions, we could discern clear differences in MT-directed activities of Op18 derivatives. As shown in Fig. 7, injection of Op18-wt and the COOH-terminal–truncated derivative (Op18-Δ100-147) resulted in loss of MTs from the lamella. While a few long MTs continued to extend out towards the cell surface, many MTs appeared shorter and did not enter the lamella region. In contrast, the NH_2-terminal truncations (Op18-Δ5-9 and Op18-Δ5-25) had less effects, but some loss of MT polymer was observed.

The loss of MTs from the lamellar region, which most likely reflect shortened MTs, provided a clear morphological assay to compare the phenotype of Op18 derivatives. We measured the number of cells that exhibited 25% or more of the lamella region cleared of MTs. The results are summarized in Fig. 8 and show that microinjection of Op18-wt resulted in a 12-fold increase in the fraction of cells with cleared lamella. The NH_2 terminally truncated proteins showed low activity, whereas the Op18-Δ100-147 protein was almost as active as the wild type. Hence, analysis of lamellar clearing indicates an overlapping phenotype of Op18-wt and the Op18-Δ100-147 derivative that is dissociated from that of the NH_2-terminal–truncated derivatives. It is notable that while the Op18-Δ5-9 derivative is significantly more efficient than Op18-Δ100-147 in de-

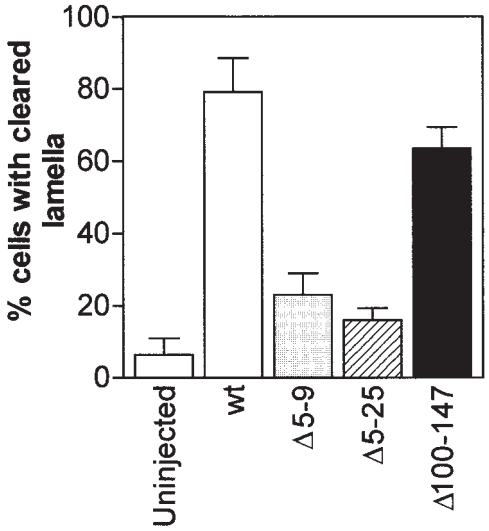

Figure 8. The lamellar clearing phenotype of microinjected newt lung cells is dependent on the extreme NH_2-terminal region of Op18. Cells were microinjected with the indicated Op18 protein derivative as in Fig. 7. The data presented were generated from 2 to 5 coverslips per Op18 derivative. The percentage of cells with 25% or more of the lamella region empty of MTs was determined from 67–245 cells per Op18 derivative. Data are means ± SD.

creasing the total MT content of K562 cells (Fig. 6), the same 4–amino acid NH_2-terminal truncation attenuates most of the lamellar clearing phenotype in newt cells (Fig. 8). These results dissociate the lamellar clearing phenotype observed in newt cells from the decrease in total MT content of K562 cells and support the idea that the NH_2- and COOH-terminal–truncated proteins in part regulates MTs by distinct mechanisms. This in turn suggests that Op18-wt has the potential to regulate the MT system by more than one specific mechanism.

Discussion

Here, we have performed a deletion analysis of Op18, the prototype member of a novel class of MT regulators, and identified regions involved in differential modulation of tubulin GTP metabolism. How these in vitro activities segregate from tubulin binding properties and specific MT-regulating activities in intact cells was determined to address the mechanism by which Op18 exerts its regulatory role. These analyses were facilitated by the maintenance of protein stability by all the truncations tested, which indicated that Op18 lacks distinct domain structures. Using these truncated Op18 proteins, physically separated tubulin binding motifs of both the NH_2- and COOH-terminal regions were found to transmit distinct tubulin-directed signals. These signals were manifested on the level of modulation of both exchange and hydrolysis of tubulin-bound GTP (Fig. 2). By analyzing the activities of deleted Op18 derivatives in K562 cells, we obtained data most consistent with MT destabilization by a mechanism other than tubulin sequestration. Hence, K562 cells contain sufficient endogenous Op18 to sequester all unpolymerized tubulin (Fig. 6 and Table III) and NH_2- and COOH-terminal deletion mutants, with decreased tubulin binding affinity, were unable to compete for tubulin binding (Fig. 5). However, despite a low level of association with cellular tubulin, these mutants still cause a drastic phenotype in intact cells (Fig. 6). Moreover, a detailed analysis of tubulin binding shows that Op18-Δ100-147 has even less potential than Op18-Δ5-25 to regulate MT polymerization by a simple sequestering mechanism (Tables I and II). Nevertheless, these two derivatives still caused a similar decrease of MT content in transfected K562 cells (Fig. 6).

Given the demonstration that tubulin sequestering is not a principal mechanism, the result in this study raises two major questions: (1) are the demonstrated region-specific in vitro activities of Op18 also manifested as distinct MT-directed activities in intact cells? (2) And if so, what is the specific role of modulation of tubulin GTP metabolism? By comparing the phenotypes mediated by Op18 derivatives in transfected K562 cells and analysis of MT morphology in microinjected newt cells (Figs. 6 and 8), it is evident that NH_2- and COOH-terminal–truncated Op18 do exert different MT-directed activities consistent with in vitro data. Moreover, given the demonstrated in vitro tubulin GTP modulatory activities of Op18 and the well established functional importance of GTP hydrolysis by tubulin (Desai and Mitchison, 1997), it seems reasonable to assume that Op18 has the potential to regulate MT assembly by its modulation of tubulin GTP status. Analysis of truncated Op18 derivatives showed distinct levels of modulation, namely inhibition of GTP exchange together with either inhibition or stimulation of GTP hydrolysis. If modulation of tubulin GTP status is central to Op18 function, it should be possible in the future to link these in vitro activities to specific MT-directed activities. However, given the observed complexity, evaluation of this possibility by segregation analysis requires design of additional mutants with a more defined spectrum of activities together with a more refined phenotypic analysis in intact cells.

A central mechanistic question is whether Op18 regulates MT assembly by modulation of the GTP status of the free tubulin pool or possibly by local regulation at the tip of the MT. Op18-mediated accumulation of free GDP–tubulin would be a potential mechanism for catastrophe promotion by Op18-wt (Caplow and Shanks, 1995). However, the Op18-Δ100-147 derivative also promotes catastrophes (Howell et al., 1999b), but has the opposite overall activity of Op18-wt, namely inhibition both of the basal- and nocodazole-stimulated GTP hydrolysis of free tubulin (Figs. 1 and 2). This excludes accumulation of free GDP–tubulin as the mechanism behind catastrophe promotion. Analysis of Op18–tubulin association, in crude cell extracts from transfected cells, provides independent evidence against regulation of MT dynamics via modulation of the free tubulin pool. The data show that endogenous native Op18 successfully competes with truncated Op18 mutants for binding to cellular tubulin (Fig. 5), which implies that these mutants exert their effect in intact cells by an alternative mechanism (Fig. 6). Hence, some of the available data are clearly incompatible with a mechanism inferring Op18 modulation of the GTP status of the free tubulin pool. While this does not exclude a potential role of Op18 modulation of the GTP-status of free tubulin, it does suggest that Op18 exerts at least part of its regulatory activity

by an alternative mechanism, such as interaction with the tips of MTs. A finding in favor to such a mechanism is that Op18 promotes catastrophes only from the plus end of MTs (Howell et al., 1999), the end where the E site GTP of β-tubulin is exposed (Nogales et al., 1999), which hints to an MT end–specific activity that may involve GTP hydrolysis at the tip. As would be predicted from a requirement for GTP hydrolysis, it has been shown that Op18 does not depolymerize MTs capped with tubulin containing the nonhydrolyzable GTP analogue guanylyl (α, β)-methylene diphosphonate (Howell et al., 1999). Given the evidence of plus end specificity and involvement of GTP hydrolysis, it is clear that Op18 acts by a different mechanism from that demonstrated for another class of catastrophe promoters, exemplified by XKCM1 and XKIF2, which act at both ends of MTs by inducing a conformational change that does not involve GTP hydrolysis (Desai et al., 1999; McNally, 1999).

Here, we show that Op18 retains significant tubulin binding after extensive deletions and the data demonstrate that Op18 binds tubulin heterodimers via multiple nonessential contacts that span residue 9 through the major part of the Op18 polypeptide (Tables I and II). It is notable that all tubulin binding Op18 derivatives (i.e., all derivatives except Op18-Δ5-55) also manifest one or more levels of tubulin-directed modulation of GTP metabolism (Fig. 1). Our data show that Op18 binds tubulin according to a two-site cooperative binding model, which implies that binding of the first tubulin creates a high affinity binding site for the second tubulin (Figs. 3 and 4). Hence, tubulin–tubulin interactions may be important for generation of the second binding site. This raises the possibility that some of the demonstrated tubulin-directed activities of Op18 are generated by Op18-promoted tubulin dimerization. However, two lines of evidence indicate that this is not sufficient for stimulation of GTPase activity. First, such a mechanism predicts that increasing Op18 concentrations (i.e., well above K_d1; Table II), which favors Op18 binding to a single tubulin, would eventually lead to inhibition of tubulin GTPase activity. However, Op18 dose responses up to 60 μM, using 5 μM tubulin both in the presence or absence of glycerol, fail to reveal high dose inhibition of tubulin GTPase activity (data not shown). Second, we have recently reported that two classes of Op18 mutants dissociate tubulin binding from stimulation of GTPase activity (Larsson et al., 1999). One class was mutated in heptad repeats of hydrophobic residues and the other involved substitution of phosphorylation sites to negatively charged glutamic acid residues. The resulting mutants showed a comparable decrease in their tubulin binding, but only the class of mutants with exchange of hydrophobic residues were defective in stimulation of tubulin GTPase activity. Hence, although Op18-promoted tubulin–tubulin interactions may be functionally important, it is evidently not sufficient for Op18-mediated stimulation of GTPase activity.

In a previous in vitro study of MT assembly (Howell et al., 1999b), the Op18-Δ5-25 and Op18-Δ100-147 derivatives were used to show that the catastrophe promoting activity of Op18 requires the NH_2-terminal region of Op18, whereas a polymerization rate inhibiting activity requires the COOH-terminal region. We proposed that a tight tubulin complex formed by either Op18-wt or Op18-Δ5-25 inhibited the polymerization rate by tubulin sequestering. Under the conditions used for both derivatives, inhibition of the tubulin polymerization rate was only observed at pH 6.8 and not at 7.4. At the time, this was readily explained by the reported increase of Op18–tubulin binding at the lower pH. In this study, we determined binding affinities of Op18-wt and Op18-Δ5-25 at pH 6.8 and 7.4, using the same conditions as during MT assembly (i.e., PEM buffer in the absence of glycerol; Table II). It is evident that tubulin binding of Op18-Δ5-25 at pH 6.8 is essentially the same as Op18-wt binding at pH 7.4. Hence, assuming a simple sequestering mechanism, the present binding data predict that the polymerization inhibitory activity of Op18-wt at pH 7.4 should be similar to the activity of Op18-Δ5-25 at pH 6.8. This was clearly not the case since these two derivatives showed indistinguishable polymerization inhibitory activity at pH 6.8 and none showed inhibition at pH 7.4 (Howell et al., 1999b). These results show that the pH sensitive Op18 inhibition of polymerization rates cannot be explained by a sequestering mechanism as proposed by us and others (Curmi et al., 1997; Howell et al., 1999b) and that a more specific pH-regulated mechanism must be involved.

The in vitro study discussed above (Howell et al., 1999b) shows that the Op18-Δ100-147 derivative promotes catastrophes at both pH 6.8 and 7.4 without a detectable inhibition of the polymerization rate. It is notable that this derivative was found here to be almost as efficient as Op18-wt in causing the observed lamellar clearing phenotype in newt cells (Figs. 5 and 6). This phenotype is diagnostic for shortening of MTs and is the predicted phenotype of a specific catastrophe promoting factor. This supports the physiological significance of the catastrophe activity of specific Op18 derivatives observed in vitro. However, although Op18 is versatile with respect to modulation of GTP metabolism of free tubulin, more work is required to deduce the mechanism by which Op18 regulates MT dynamics.

We thank V. Shingler (University of Umeå) for helpful discussions.

N. Larsson, B. Segerman, K. Fridell, and M. Gullberg were supported by Swedish Natural Science Research Council and the Foundation for Medical Research at the University of Umeå. B. Howell and L. Cassimeris were supported by a National Institutes of Health grant.

Submitted: 18 June 1999
Revised: 10 August 1999
Accepted: 12 August 1999

References

Austin, S., and R. Dixon. 1992. The prokaryotic enhancer binding protein NTRC has an ATPase activity which is phosphorylation and DNA dependent. *EMBO (Eur. Mol. Biol. Organ.) J.* 11:2219–2228.

Belmont, L.D, and T.J. Mitchison. 1996. Identification of a protein that interacts with tubulin dimers and increases the catastrophe rate of microtubules. *Cell.* 84:623–631.

Brattsand, G., G. Roos, U. Marklund, H. Ueda, G. Landberg, E. Nanberg, P. Sideras, and M. Gullberg. 1993. Quantitative analysis of the expression and regulation of an activation-regulated phosphoprotein (oncoprotein 18) in normal and neoplastic cells. *Leukemia.* 7:569–579.

Brylawski, B.P., and M. Caplow. 1983. Rate for nucleotide release from tubulin. *J. Biol. Chem.* 258:760–763.

Caplow, M., and J. Shanks. 1995. Induction of microtubule catastrophe by formation of tubulin-GDP and apotubulin subunits at microtubule ends. *Biochemistry.* 34:15732–15741.

Cassimeris, L. 1999. Accessory protein regulation of microtubule dynamics

throughout the cell cycle. *Curr. Opin. Cell Biol.* 11:134–141.
Curmi, P.A., S.S. Andersen, S. Lachkar, O. Gavet, E. Karsenti, M. Knossow, and A. Sobel. 1997. The stathmin/tubulin interaction in vitro. *J. Biol. Chem.* 272:25029–25036.
Deacon, H.W., T.J. Mitchison, and M. Gullberg. 1999. Op18/stathmin. *In* Guidebook to the Cytoskeletal and Motor Proteins. T. Kreis and R. Vale, editors. Oxford University Press, Oxford. In press.
Desai, A., and T.J. Mitchison. 1997. Microtubule polymerization dynamics. *Annu. Rev. Cell Dev. Biol.* 13:83–117.
Desai, A., S. Verma, T.J. Mitchison, and C.E. Walczak. 1999. Kin I kinesins are microtubule-destabilizing enzymes. *Cell.* 96:69–78.
Gard, D.L., and M.W. Kirschner. 1987. Microtubule assembly in cytoplasmic extracts of *Xenopus* oocytes and eggs. *J. Cell Biol.* 105:2191–2201.
Gavet, O., S. Ozon, V. Manceau, S. Lawle, P. Curmi, and A. Sobel. 1998. The stathmin phosphoprotein family: intracellular localization and effects on the microtubule network. *J. Cell Sci.* 22:3333–3334.
Gradin, H.M., U. Marklund, N. Larsson, T.A. Chatila, and M. Gullberg. 1997. Regulation of microtubule dynamics by Ca^{2+}/calmodulin-dependent kinase IV/Gr-dependent phosphorylation of oncoprotein 18. *Mol. Cell Biol.* 17: 3459–3467.
Gradin, H.M., N. Larsson, U. Marklund, and M. Gullberg. 1998. Regulation of microtubule dynamics by extracellular signals: cAMP-dependent protein kinase switches off the activity of oncoprotein 18 in intact cells. *J. Cell Biol.* 140:131–141.
Graessmann, A., M. Graessmann, and C. Mueller. 1980. Microinjection of early SV40 DNA fragments and T antigen. *Methods Enzymol.* 65:816–825.
Gundersen, G.G., and T.A. Cook. 1999. Microtubules and signal transduction. *Curr. Opin. Cell Biol.* 11:81–94.
Howell, B., D.J. Odde, and L. Cassimeris. 1997. Kinase and phosphatase inhibitors cause rapid alterations in microtubule dynamic instability in living cells. *Cell. Motil. Cytoskeleton.* 38:202–214.
Howell, B.J., H. Deacon, and L. Cassimeris. 1999a. Decreasing oncoprotein 18 levels reduce microtubule catastrophes and increase microtubule polymer in vivo. *J. Cell Sci.* In press.
Howell, B., N. Larsson, M. Gullberg, and L. Cassimeris. 1999b. Dissociation of the tubulin-sequestering and microtubule catastrophe-promoting activities of oncoprotein 18/stathmin. *Mol. Biol. Cell.* 10:105–118.
Jourdain, L., P. Curmi, A. Sobel, D. Pantaloni, and M.F. Carlier. 1997. Stathmin: a tubulin-sequestering protein which forms a ternary T2S complex with two tubulin molecules. *Biochemistry.* 36:10817–10821.
Koshland, D.E., Jr., G. Nemethy, and D. Filmer. 1966. Comparison of experimental binding data and theoretical models in proteins containing subunits. *Biochemistry.* 5:365–385.
Larsson, N., H. Melander, U. Marklund, O. Osterman, and M. Gullberg. 1995. G2/M transition requires multisite phosphorylation of oncoprotein 18 by two distinct protein kinase systems. *J. Biol. Chem.* 270:14175–14183.
Larsson, N., U. Marklund, H.M. Gradin, G. Brattsand, and M. Gullberg. 1997. Control of microtubule dynamics by oncoprotein 18: dissection of the regulatory role of multisite phosphorylation during mitosis. *Mol. Cell Biol.* 17: 5530–5539.
Larsson, N., B. Segerman, H.M. Gradin, E. Wandzioch, L. Cassimeris, and M. Gullberg. 1999. Mutations of oncoprotein 18/stathmin identify tubulin-directed regulatory activities distinct from tubulin association. *Mol. Cell Biol.* 19:2242–2250.
Marklund, U., O. Osterman, H. Melander, A. Bergh, and M. Gullberg. 1994. The phenotype of a "Cdc2 kinase target site-deficient" mutant of oncoprotein 18 reveals a role of this protein in cell cycle control. *J. Biol. Chem.* 269: 30626–30635.
Marklund, U., N. Larsson, H.M. Gradin, G. Brattsand, and M. Gullberg. 1996. Oncoprotein 18 is a phosphorylation-responsive regulator of microtubule dynamics. *EMBO (Eur. Mol. Biol. Organ.) J.* 15:5290–5298.
McNally, F.J. 1999. Microtubule dynamics: controlling split ends. *Curr. Biol.* 9:R274–R276.
Minotti, A.M., S.B. Barlow, and F. Cabral. 1991. Resistance to antimitotic drugs in Chinese hamster ovary cells correlates with changes in the level of polymerized tubulin. *J. Biol. Chem.* 266:3987–3994.
Nogales, E., M. Whittaker, R.A. Milligan, and K.H. Downing. 1999. High-resolution model of the microtubule. *Cell.* 96:79–88.
Ozon, S., A. Maucuer, and A. Sobel. 1997. The stathmin family—molecular and biological characterization of novel mammalian proteins expressed in the nervous system. *Eur. J. Biochem.* 248:794–806.
Rieder, C.L., and R. Hard. 1990. Newt lung epithelial cells: cultivation, use, and advantages for biomedical research. *Int. Rev. Cytol.* 122:153–220.
Riederer, B.M., V. Pellier, B. Antonsson, G. Di Paolo, S.A. Stimpson, R. Lutjens, S. Catsicas, and G. Grenningloh. 1997. Regulation of microtubule dynamics by the neural growth-associated protein SCG10. *Proc. Natl. Acad. Sci. USA.* 94:741–745.
Saxton, W.M., D.L. Stemple, R.J. Leslie, E.D. Salmon, M. Zavortink, and J.R. McIntosh. 1984. Tubulin dynamics in cultured mammalian cells. *J. Cell Biol.* 99:2175–2186.